

Supporting Information

Krause et al. 10.1073/pnas.0914360107

SI Experimental Procedures

Agonists and Antagonists. Troglitazone, rosiglitazone, pioglitazone, ciglitazone, GW9662, and BIO were acquired commercially (Calbiochem). Dkk-1 was prepared from a recombinant source as described (1).

Tissue Culture. Human MSCs were cultured in α -MEM (Invitrogen, Carlsbad, CA) containing 20% (vol/vol) FBS (Atlanta Biologicals), 100 units·mL⁻¹ penicillin, 1 μ g·mL⁻¹ streptomycin, and 4 mM L-glutamine. For expansion, cells were plated at an initial seeding density of 100 cells/cm² and allowed to divide for six to eight doublings until 40–50% confluent. For repassage and experiments, MSCs were recovered with trypsin/EDTA mixture (Invitrogen).

ALP Assays. Osteoblastogenesis was induced on confluent monolayers in 6- to 24-well plates by addition of complete culture medium supplemented with 5 mM sodium glycerophosphate and 50 μ g·mL⁻¹ L-ascorbate. Inhibitors were added to the conditions where appropriate (acquired from Calbiochem, San Diego, and Sigma Aldrich). Medium was changed every 48 h. After 8–10 days, a measurement of ALP activity was to be carried out on the monolayers. The cells were washed once with PBS, then with 100 mM Tris-HCl (pH 9.0) containing 100 mM KCl and 1 mM MgCl₂ (ALP buffer). After washing, 1.5 mL of a 1:2 solution of PNPP (Fisher) and ALP buffer was added to the wells to produce a 5-mm path length between the bottom of the well and the meniscus. ALP activity as a function of PNPP metabolism (Δ OD₄₀₅ min⁻¹) was measured by using a temperature-controlled automated plate reader (FluoStar; BMG Biotech). The rates were compared against standards with a known concentration of ALP and normalized against cell number.

Cell Cycle Assays. Cells were recovered by trypsinization, rinsed in PBS, and fixed for 4 h in 70% (vol/vol) ethanol. Pellets were then resuspended in PBS containing 0.1% (wt/vol) BSA (Sigma), 20 mg·mL⁻¹ RNase A (Invitrogen), and 50 mg·mL⁻¹ propidium iodide (Sigma). Profiles were generated by fluorescent activated cell sorting (Becton Coulter FC500) and analyzed with modeling software (MultiCycleAV; Phoenix Flow Systems).

Microarray Processing. RNA quality and quantity was determined with capillary electrophoresis (Experion; Bio-Rad) by using RNA Nano Kit (Bio-Rad). Total of 1.4–4.0 μ g of total RNA was used for one-cycle target labeling assay according to manufacturer's instructions (Affymetrix). Briefly, Poly-A RNA spike in controls were added to each sample, and double-stranded cDNA was synthesized by using One-Cycle cDNA Synthesis Kit (Affymetrix). Double-stranded cDNA was cleaned with Sample Cleanup Module (Affymetrix) followed by synthesis of biotin-labeled cRNA using the GeneChip IVT Labeling Kit (Affymetrix). Biotin-labeled cRNA was cleaned with Sample Cleanup Module and quantified with spectrophotometer (SmartSpec; Bio-Rad). A total of 20 μ g of biotin-labeled cRNA was used for fragmentation by using the Sample Cleanup Module. The labeled and fragmented cRNA was hybridized on to HG-U133 Plus 2.0 (Affymetrix) arrays with hybridization controls from the GeneChip Hybridization, Wash, and Stain Kit (Affymetrix) in Hybridization Oven 450 (Affymetrix). After 16 h of hybridization, the arrays were washed and stained in Fluidics Station 450 (Affymetrix) by using the GeneChip Hybridization, Wash, and Stain Kit. The arrays were then scanned by using the GeneChip Scanner G7 (Affymetrix). Command Console (Affymetrix) software was used to run the instruments and perform quality control of the samples.

Microarray Data Analysis. The microarray image files (CEL files) were transferred to Partek Genomics Suite (Partek) for data analysis. The arrays were normalized by using RMA (robust multichip analysis) algorithm. The data were filtered by comparing each array to DMSO control and keeping the genes that showed at least 2-fold up- or down-regulation in their expression level. The lists of genes were also studied for GeneOntology enrichment. All of the differentially expressed genes (5,077 genes) were combined into one list and their gene expression values were standardized, and used for hierarchical clustering. Eight clusters were selected on the same level of hierarchy (distance 1.4–1.6) and studied for GeneOntology enrichment.

ELISA. ELISA for CXCL6, Dkk-1, GRO α , GRO β , and OPG were carried out by using nonbiotinylated polyclonal capture antibodies and biotinylated detection antibodies that were commercially acquired (R&D Systems and PromoKine) on Nunc Immunosorp coated 96-well plates (Fisher Lifesciences). The biotinylated capture antibodies were detected by using horseradish peroxidase-conjugated streptavidin and TMB substrate (Pierce). ELISA for IL-1b were performed by using commercially acquired kits.

Antibody Array. Microarray data of secreted cytokines were confirmed by using a membrane-based antibody array to test for the relative concentrations of 174 proteins as recommended by the manufacturer (RayBio Human Cytokine Array; RayBiotech). In brief, culture supernatants from 8-day drug- or vehicle-treated MSCs were collected from two donors after 24 h. Membranes were blocked and incubated with 3 mL of supernatant each overnight on an orbital shaker at 4 °C. After washing, membranes were incubated with biotinylated antibodies for 3 h at room temperature and developed by using streptavidin-conjugated horseradish peroxidase and an ECL substrate. Chemiluminescence was detected on a Versadoc Imaging System and analyzed by using QuantityOne software (Bio-Rad). After local background subtraction, the mean volume of duplicate spots for each protein was normalized to the average volume of the six internal positive controls on each membrane. Data are expressed as relative intensity values. Membranes incubated with culture medium containing 20% (vol/vol) FBS showed negligible background cross-reactivity.

Cell Counting. Cells were recovered by trypsinization and pelleted. The number of cells per well were then measured by nucleic acid fluorescence incorporation assay. The cells were added to 2 \times CyQuant dye solution (Invitrogen) containing 1 unit per mL of EcoRI and BamHI (Invitrogen) to lyse the cells and release the DNA from the protein. Nucleic acid interchelation-induced fluorescence was measured by using a microplate fluorescence reader (FLx800; Bio-Tek Instruments) set to 480-nm excitation and 520-nm emission. The degree of fluorescence is directly proportional to cell number when compared against known standards.

Late-Stage Osteogenesis and Alizarin Red Staining. Confluent cultures of MSCs were incubated in complete osteogenic medium consisting of osteogenic base media containing 10⁻⁸ M dexamethasone (Sigma) with the appropriate inhibitor or vehicle. Media was changed every 2 days until the conclusion of the assay. Alizarin red staining, back extraction, and quantification were performed as described (2) Stained monolayers were photographed by using a Nikon Eclipse TE200 inverted microscope fitted with a Nikon DXM1200F digital camera.

Western Blotting Antibodies. The following antibodies were used: mouse anti-human GAPDH (clone 6C5; Chemicon International), mouse anti-human β -catenin (clone 5H10; Chemicon), mouse anti-human GSK3 β (clone M131; Abcam), PPAR gamma (clone 1E6A1; Abcam), and rabbit anti-cleaved caspase 3 (Abcam). Secondary antibodies were goat anti-mouse Ig-peroxidase conjugate and goat anti-rabbit peroxidase conjugate (Fisher Lifesciences). Film development was carried out as previously described (3). Silver staining was performed by using a commercially available kit (Invitrogen).

Clotted Plasma Coculture. Confluent monolayers of MSCs were generated in wells of a 12-well tissue culture plate. Clotting human plasma was prepared by suspending freeze-dried human plasma (Sigma) to 2 \times concentration and combining the solution with an equal volume of 1 \times thromboplastin C (Fisher Lifesciences). To slow clotting, the components and mixture was maintained on ice. Media was removed from the confluent cultures, washed in PBS and, with the plates held at an angle of $\approx 20^\circ$, 200 μ L of the plasma mixture was added to each well so as to cover $\approx 30\%$ of the surface area. After the plasma had clotted (5 min), osteogenic media was carefully added to cover the monolayer and plasma. Osteogenic assays were then performed by using standard media preparations.

Calvarial Lesions. MSCs were cultured in the presence of osteogenic base media containing the appropriate inhibitor or vehicle with media changes every 2 days. After 8 days of in vitro conditioning, they were recovered, suspended in commercially acquired human plasma at 20 million cells per mL. Under an institutionally approved animal use protocol, nude mice (Jackson Laboratories) received a 3-mm circular lesion in the frontal or parietal calvarial bones, 1–2 mm from the sagittal and coronal sutures. The chilled cell suspension (50 μ L) was added to an equal volume of thromboplastin and administered to the lesion. After clotting, the scalp was to be closed by suture and tissue glue. Subsequent doses of cells were administered by direct injection in plasma/thromboplastin mix.

X-Ray Imaging and Quantification. In accordance with an institutionally approved animal use protocol, cranial bones were dissected out of euthanized mice and gently cleared of connective tissue. The bones were imaged by x-ray (Faxitron M20) with a 30-KV beam for 15 s. Digital images were to be captured on a digital plate and processed on a PhosphorImager reader (PMI; Bio-Rad). Images were processed by volume analysis software (Quantity One; Bio-Rad). The degree of radio-opacity at comparable regions of interest on the lesioned and contralateral side was defined as the reciprocal of the pixel volume intensity. Results were presented as the percent radio-opacity at the lesion with the unaffected contralateral side set to 100 percent.

Histochemistry and Immunocytochemistry. For nuclear localization studies, hMSCs were fixed in 4% (vol/vol) paraformaldehyde for 15 min and blocked/permeabilized in PBS containing 2% (vol/vol) goat serum (Sigma) and 0.1% (vol/vol) Triton X-100. A cy-3 labeled monoclonal antibody (clone 15B8; Sigma) was used to detect β -catenin, and nuclei were counterstained with Pico green DNA dye (Invitrogen).

Calvaria were fixed in 4% (wt/vol) paraformaldehyde for 15 h, then decalcified for 48 h in PBS containing 1 M disodium-EDTA (EDTA). Specimens were then washed three times with 50 mL of PBS for 2 h at 4 $^\circ$ C. Specimens were processed as paraffin blocks and 8- μ m longitudinal sections were prepared, deparaffinized, and rehydrated, then stained with hematoxylin and eosin (Sigma). For immunocytochemistry, rehydrated sections were treated with 3% (vol/vol) hydrogen peroxide for 15 min at room temperature, washed in PBS, then blocked in PBS containing 2% (vol/vol) goat serum (Sigma) and 0.1% (vol/vol) Triton X-100. An anti-human β -2-microglobulin antibody was employed to detect human cells (Abcam, Cambridge, MA). Secondary detection was achieved by using the Alexafluor series of antibodies. An upright fluorescent microscope (Eclipse H600L; Nikon) fitted with a high performance camera (Retiga 2000R), and image analysis software (NIS-Elements; Nikon) was employed for imaging.

Tetracycline Tracing of in Vivo Calcium Deposition. Animals received s.c. injections of tetracycline (25 mg/kg) 10 days before euthanasia in accordance with an institutionally approved animal use protocol. After fixation under vacuum and agitation, the specimens were dehydrated in several changes of graded EtOH solutions and cleared with xylenes and then 100% methyl methacrylate (MMA). Specimens were then infiltrated for ≈ 2 weeks under vacuum with three solutions of MMA and dibutyl phthalate (DBP). After the infiltration period, the specimens were then embedded in a fresh solution of MMA + DBP + Perkadox-16 (P16). Using the combination of room temperature, a refrigerator, a waterbath, and an oven, the specimens were allowed to polymerize (harden) over a period of ≈ 3 –5 days. Thin-section microtomy (5 microns) was performed by using a motorized rotary microtome (Leica Microsystems) and a tungsten-carbide knife (Dorn and Hart Microedge). Sections were then deplasticized and visualized by using an upright fluorescent microscope (Eclipse H600L; Nikon) fitted with a high performance camera (Retiga 2000R) and image analysis software (NIS-Elements; Nikon) was employed for imaging. Embedding, sectioning, and mounting was outsourced to J. L. Ratcliff (Franklin, TN).

Semiquantitative Blood Vessel Measurements. Calvaria were fixed, decalcified, and sectioned in paraffin and stained with hematoxylin and eosin as described. Two-dimensional regions of interest (ROI) were carefully defined and normalized for all specimens. For this purpose, 6- μ m-thick longitudinal serial sections were prepared, and those sections containing tissue up to and including 0.5 mm above and below the diameter of the lesion. These were included in the measurements. A 6- μ m section was counted every 30 μ m (34 sections) within the entire region of interest, which consisted of the longitudinal thickness of the lesion (the thickness of the bone and adjacent fibrous tissue) by the original width of the lesion in one dimension (3 mm) and 0.5 mm above and below the original diameter of the lesion in the final dimension. Using NIS-Elements image analysis software, the surface area of blood vessels in the 2D ROI was calculated for each section and totaled. The values were expressed as the mean of total blood vessel area from three animals per group.

1. van der Horst G, et al. (2005) Downregulation of Wnt signaling by increased expression of Dickkopf-1 and -2 is a prerequisite for late-stage osteoblast differentiation of KS483 cells. *J Bone Miner Res* 20:1867–1877.
2. Gregory C-A, Gunn W-G, Peister A, Prockop D-J (2004) An Alizarin red-based assay of mineralization by adherent cells in culture: comparison with cetylpyridinium chloride extraction. *Anal Biochem* 329:77–84.

3. Damiens E, Baratte B, Marie D, Eisenbrand G, Meijer L (2001) Anti-mitotic properties of indirubin-3'-monoxime, a CDK/GSK-3 inhibitor: induction of endoreplication following prophase arrest. *Oncogene* 20:3786–3797.

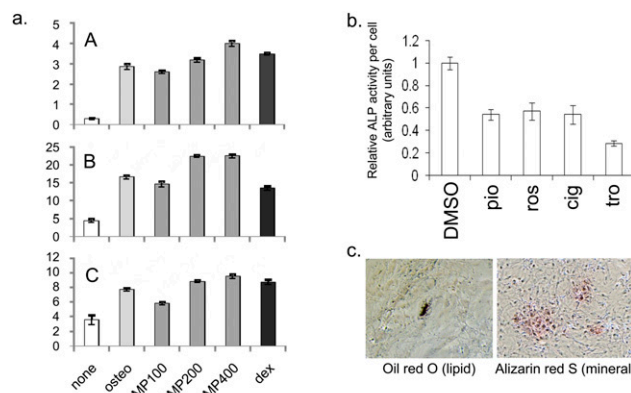


Fig. S1. Effect of β -glycerophosphate and ascorbic acid, BMP2, dexamethasone, and various PPAR γ agonists on osteogenesis. (A) Monolayers of hMSCs from 3 donors (A, B, and C) were exposed to complete media (CCM), CCM with osteogenic base supplements, 5 mM β -glycerophosphate, and 50 $\mu\text{g}\cdot\text{mL}^{-1}$ ascorbic acid (OBM), OBM with various concentrations (in $\text{ng}\cdot\text{mL}^{-1}$), bone morphogenetic protein 2 (BMP2), and dexamethasone (10^{-8} M). Note that the ALP levels are substantially raised by OBM treatment and can be improved further by high concentrations of BMP2 ($n = 3$). (B) Effect of 50 μM of various PPAR γ agonists on ALP activity measured by colorimetric assay. All values were normalized to cell number. Data are expressed as means with standard deviations ($n = 6$). Pioglitazone (pio), rosiglitazone (ros), ciglitazone (cig), and troglitazone (tro). (C) In the presence of high concentrations of PPAR γ agonists, osteogenic cultures of hMSCs initiate adipogenesis rather than osteogenesis. After 20 days of differentiation in OBM containing 10^{-8} M dex and 10 μM troglitazone, cultures show Oil Red O-positive lipid islands and only weak mineralization (ARS staining).

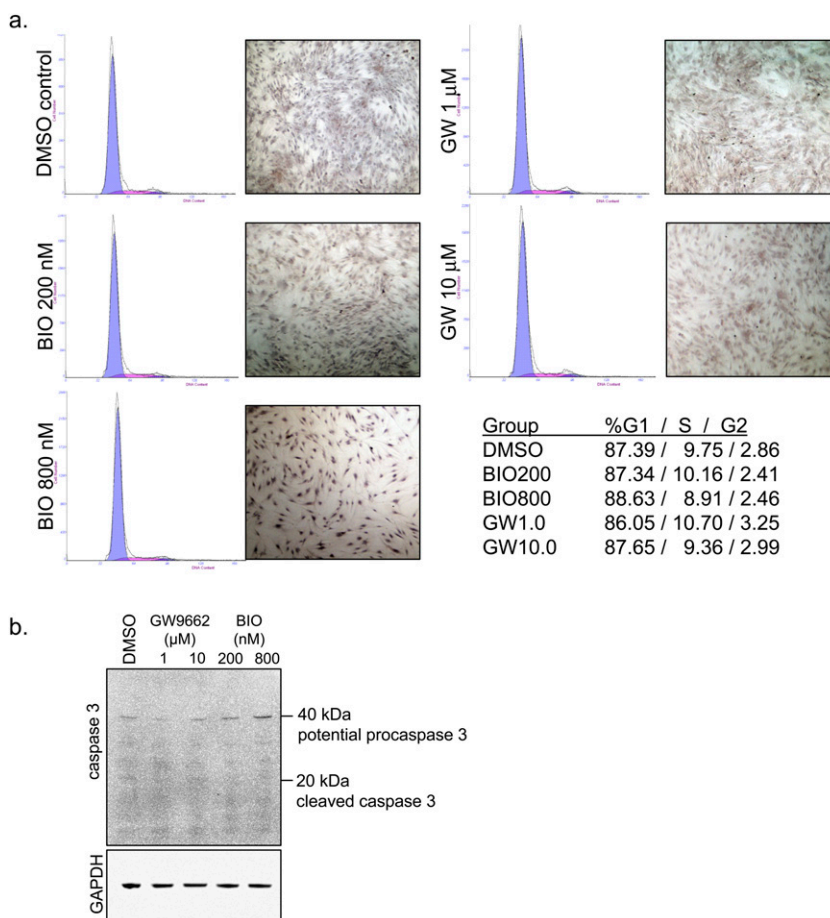


Fig. S2. Cell cycle analysis of vehicle, BIO-, and GW-treated cells after 8 days in culture. (A) DNA content was measured by propidium iodide incorporation, followed by fluorescent activated cell sorting. All cultures had similar cell cycle profiles, with the predominant population in G $_1$, suggesting a degree of contact inhibition. Although cells treated with 800 nM BIO were semiconfluent, the cell cycle status of these hMSCs was similar to the other groups, suggesting cell cycle inhibition that was not related to culture density. Representative cultures of control, BIO-, and GW-treated cells counterstained with eosin are presented with the cell cycle profiles to demonstrate the relative culture densities. (B) Immunoblots of cleaved caspase-3 (Asp175) on whole cell extracts of hMSCs treated with BIO or GW. There is no evidence of caspase 3 processing. Note the potential cross reactivity with procaspase 3. Blots were normalized with GAPDH.

Table S2. Gene ontology categorization of up-regulated genes in GW9662- and BIO-treated hMSCs

Function	Score
Membrane part	27.5164
Intrinsic to membrane	26.0127
Integral to membrane	23.6473
RNA binding	20.2434
RNA processing	19.4775
RNA metabolic process	18.9374
mRNA processing	18.3935
Membrane	17.8623
Receptor activity	16.5981
mRNA metabolic process	16.1985
Nuclear body	16.0694
Intracellular part	15.3647
Transmembrane receptor activity	15.2685
Regulation of Ras GTPase activity	15.2184
Regulation of GTPase activity	14.6535
Nucleoplasm part	14.2069
Nuclear part	13.7130
Intracellular organelle	13.5684
RNA splicing	13.4278
Signal transducer activity	13.3653
Molecular transducer activity	13.3653
Nuclear mRNA splicing, via spliceosome	13.3446
Regulation of ARF GTPase activity	13.2798
Nucleotide binding	13.1939
Collagen	13.1052
GTPase activator activity	12.9198
ARF GTPase activator activity	12.7744
G protein coupled receptor protein signaling pathway	12.0761
Protein localization	12.0587
GTPase regulator activity	11.8750
Response to stimulus	11.8577
G protein coupled receptor activity	11.7330
Macromolecule localization	11.4025
Cellular macromolecule metabolic process	11.3837
Nuclear speck	11.3583
Nucleus	11.3502
Ras GTPase activator activity	11.0715
Plasma membrane	11.0066
Immune response	10.9736
Cytoplasm	10.8964
Muscle thin filament tropomyosin	10.7406
Protein binding	10.7210
Intrinsic to plasma membrane	10.7024
Protein farnesyltransferase activity	10.3374
Protein amino acid farnesylation	10.3374
Hemidesmosome	10.3374
Integral to plasma membrane	10.3207
Cellular protein metabolic process	10.1287
Biopolymer metabolic process	9.86304
Rhodopsin-like receptor activity	9.82835
Extracellular region	9.67791
Intracellular membrane-bounded organelle	9.62580
Macromolecule metabolic process	9.45201
Protein modification process	9.20919
Plasma membrane part	9.08948
Intracellular transport	9.01389
Ubiquitin-protein ligase activity	8.89770
Acid-amino acid ligase activity	8.72389
Zinc ion binding	8.68187
Small conjugating protein ligase activity	8.47253
Neuromuscular junction development	8.26452
Cellular_component	8.15432

Table S2. (Cont.)

Function	Score
Transmembrane transporter activity	8.14914
NADPH:quinone reductase activity	8.11148
Polytene chromosome chromocenter	8.11148
Negative regulation of Rho protein signal transduction	8.11148
Establishment of localization in cell	8.01233
ATP-dependent helicase activity	7.89262
Binding	7.74701
Transporter activity	7.71191
Heterogeneous nuclear ribonucleoprotein complex	7.57409
Golgi to endosome transport	7.36078
Wnt receptor signaling pathway through beta-catenin	7.36078
Nucleic acid binding	7.21703
Posttranslational protein modification	7.18282
Regulation of small GTPase mediated signal transduction	7.13642
Metal ion transport	7.13251
Ligase activity, forming carbon-nitrogen bonds	7.00821
Localization	6.80309
Mediator complex	6.78123
Transition metal ion binding	6.77774
Ubiquitin-dependent protein catabolic process	6.74139
Extracellular space	6.64369
Double-stranded DNA binding	6.62313
Polynucleotide adenyltransferase activity	6.61480
Farnesyltransferase activity	6.61480
Receptor tyrosine kinase binding	6.61480
Beta-N-acetylhexosaminidase activity	6.61480
Vesicle	6.61480
Organelle	6.61480
Protein import into mitochondrial matrix	6.61480
Fibrillar collagen	6.60614
Camera-type eye morphogenesis	6.60614
Modification-dependent protein catabolic process	6.54899
Multicellular organismal process	6.49879
Channel activity	6.48427

Enrichment scores are derived from *P* values ($10^{\text{enrichment score}} = P$ value against the probability that a given gene clustered based on chance alone).

Table S3. Collagens and extracellular matrix components

Protein	Gene	Accession No.	Fold changes				Major location/function
			BIO200	BIO800	GW1	GW10	
<i>Collagen Ia1</i>	<i>COL1A1</i>	217430_x_at	2.75	2.79	2	3	Abundant in bone
<i>Collagen Ia1</i>	<i>COL1A1</i>	202311_s_at	2.36	2.2	2.05	2.25	
<i>Collagen Ia2</i>	<i>COL1A2</i>	225664_at	2.38	1.88	1.79	3.93	Abundant in bone
<i>Collagen IIIa1</i>	<i>COL3A1</i>	232458_at	3.12	1.22	10.4	2.8	Present in bone
Collagen IVa5	COL4A5	213110_s_at	-2.05	-2.65	-1.84	-1.29	Low/absent in bone
<i>Collagen Va3</i>	<i>COL5A3</i>	52255_s_at	1.91	1.12	1.52	3.34	Present/low in bone
<i>Collagen VI a1</i>	<i>COL6A1</i>	212091_s_at	1.92	1.66	1.85	3.23	Present in bone
<i>Collagen VI a1</i>	<i>COL6A1</i>	212940_s_at	2.05	1.66	1.14	2.99	
<i>Collagen VI a2</i>	<i>COL6A2</i>	209156_s_at	1.96	1.91	2.38	2.71	Present in bone
<i>Collagen VIIIa1</i>	<i>COL8A1</i>	221152_at	1.42	1.12	4.07	1.57	Low in bone
<i>Collagen VIIIa2</i>	<i>COL8A2</i>	52651_at	2.12	2.43	1.14	1.24	Low in bone
<i>Collagen Xa1</i>	<i>COL10A1</i>	217428_s_at	1.65	2.18	1.37	1.47	Present in mature bone
Collagen XIa1	COL11A1	229271_x_at	-1.54	-1.02	2.28	5.01	Cartilage restricted
Collagen XIa1	COL11A1	37982_at	-2.2	-3.29	5.57	4.02	
<i>Collagen XIIa1</i>	<i>COL12A1</i>	231766_s_at	2.38	1.88	1.79	3.93	Present in bone
<i>Collagen XIIa1</i>	<i>COL12A1</i>	225664_at	1.5	1.29	1.23	2.79	
<i>Collagen XIIa1</i>	<i>COL12A1</i>	231879_at	2.11	1.62	1.13	4	
Collagen XIVa1	COL14A1	212865_s_at	-3.47	-4.59	-2.28	2.2	Marrow stroma
<i>Collagen XVa1</i>	<i>COL15A1</i>	203477_at	-1.83	-2.25	2.03	2.04	Some osteoblasts
Aggrecan	ACAN	217161_x-at	1.09	1.2	1.3	2.7	Cartilage restricted
Fibronectin	FN1	1558199_at	1.88	1.87	7.29	2.6	Synthesizing bone

Bone-related collagens are italicized in the first two columns; high abundance bone-related collagens are bold. Significant fold increases are presented in bold in columns 4–6; significant fold decreases are presented in italic.

Table S4. Gene ontology categorization of down-regulated genes in GW9662- and BIO-treated hMSCs

Function	Score
Highly down-regulated in BIO-treated MSCs, moderately down-regulated in GW9662-treated MSCs.	
Thrombin receptor activity	28.0695
Trans-1,2-dihydrobenzene-1,2-diol dehydrogenase activity	28.0695
3-Alpha-hydroxysteroid dehydrogenase (A-specific) activity	22.5322
Prostanoid metabolic process	17.3850
Prostaglandin metabolic process	17.3850
Phospholipid scrambling	14.8662
Phospholipid scramblase activity	14.8662
Bile acid binding	14.8662
Acetylgalactosaminyltransferase activity	13.6365
Platelet-derived growth factor receptor activity	12.6591
Response to dsRNA	12.6591
Prostaglandin E receptor activity	12.6591
Indole and derivative metabolic process	12.6591
Indole derivative metabolic process	12.6591
Regulation of ossification	12.3625
Carboxylic acid binding	10.9963
3',5'-Cyclic-nucleotide phosphodiesterase activity	10.7854
Steroid dehydrogenase activity, acting on the CH-OH group of donors, NAD or NADP as acceptor	10.3329
Cyclic-nucleotide phosphodiesterase activity	10.3329
Adenylate kinase activity	9.69717
Integrin complex	8.79613
Highly down-regulated in GW9662 treated MSCs, moderately down-regulated in BIO-treated MSCs	
Sphingomyelin biosynthetic process	21.4244
Extracellular region	18.6676
Sphingomyelin synthase activity	16.4884
Ceramide cholinephosphotransferase activity	16.4884
Cytoplasmic part	16.1805
Stearoyl-CoA 9-desaturase activity	12.2139
Intracellular part	11.1996
Intracellular organelle part	10.5470
Y-form DNA binding	9.62809
Transcription, RNA-dependent	9.62809
Negative regulation of retroviral genome replication	9.62809
Ubiquitin-dependent protein catabolic process	9.59400
Endoplasmic reticulum	9.49858
Modification-dependent protein catabolic process	9.35670
Golgi-associated vesicle	8.89415
Signal transduction	8.86723
Extracellular region part	8.62576
Nucleosome assembly	8.59450
Protein import	8.48681
Nucleosome	8.18840
Regulation of defense response to virus by host	8.02484
Extracellular space	7.99858

Enrichment scores are derived from P values ($10^{-\text{enrichment score}} = P$ value against the probability that a given gene clustered based on chance alone).

Table S5. Gene ontology categorization of up-regulated genes in BIO-treated hMSCs

Function	Score
Positive regulation of epidermal growth factor receptor activity	83.2622
Neutrophil chemotaxis	79.0106
G protein-coupled receptor binding	68.7486
Chemokine activity	67.9314
Fever	65.5733
Chemokine receptor binding	65.4490
Regulation of protein secretion	58.0544
Epidermal growth factor receptor activating ligand activity	52.4821
Leukocyte chemotaxis	50.0283
Epidermal growth factor receptor binding	48.2312
Response to wounding	44.179
Respiratory burst	43.7386
Heat generation	43.7386
Positive regulation of phosphorylation	43.7127
Positive regulation of cell cycle	42.6954
Leukocyte migration	40.3008
Inflammatory response	40.1391
Positive regulation of phosphate metabolic process	38.4481
Regulation of interleukin-6 biosynthetic process	38.3896
Plasminogen activator activity	37.4817
Positive regulation of interleukin-6 biosynthetic process	37.4817
Macrophage chemotaxis	37.4817
Lymphocyte chemotaxis	37.4817
Induction of programmed cell death in response to chemical stimulus	33.7693
Regulation of short-term neuronal synaptic plasticity	33.7693

Enrichment scores are derived from *P* values ($10^{\text{enrichment score}} = P$ value against the probability that a given gene clustered based on chance alone).

Table S6. Inflammatory cytokine expression

Protein	Gene	Accession no.	Fold changes				Major known function	Ligand confirmed
			BIO200	BIO800	GW1	GW10		
Interleukin 1A	IL-1A	210118_s_at	2.53	2.80	<i>-2.87</i>	<i>-2.15</i>	Proinflammatory	n.d.
Interleukin 1B	IL-1B	205067_at	2.07	2.42	<i>-3.15</i>	<i>-4.40</i>	Proinflammatory	Yes
Interleukin 8	IL-8	20842_s_at	2.8	6.38	<i>-5.23</i>	<i>-6.70</i>	Proinflammatory	Yes
Interleukin 8	IL-8	202859_s_at	1.56	2.99	<i>-6.48</i>	<i>-18.97</i>		
CXC ligand 1 (GRO α)	CXCL1	204470_at	1.58	2.45	<i>-5.91</i>	<i>-8.17</i>	Neutrophil attractant	Yes
CXC ligand 2	CXCL2	209774_x_at	<i>-1.21</i>	1.31	<i>-4.49</i>	<i>-5.61</i>	Leukocyte attractant	No
CXC ligand 5 (ENA-78)	CXCL5	214974_x_at	1.03	3.6	<i>-1.08</i>	<i>-1.16</i>	Neutrophil attractant	Yes
CXC ligand 6 (GCP-2)	CXCL6	206336_at	<i>-1.25</i>	1.49	<i>-9.13</i>	<i>-5.12</i>	Neutrophil attractant	Yes
Interleukin 7	IL-7	206693_at	<i>-3.3</i>	<i>-3.19</i>	<i>-3.38</i>	<i>-3.20</i>	Lymphoid mitogen	n.d.

Significant fold increases are presented in bold in columns 4–6; significant fold decreases are presented in italic. n.d., not detected.

Table S7. Confirmation of GW9662 microarray data by ELISA

Ligand	DMSO*	GW1.0*	GW10.0*	BIO200	BIO800
IL-1 beta [†]	4.5×10^{-5}	4.5×10^{-6}	BDL	NC	NC
IL-8 [‡]	1.6×10^{-5}	3.5×10^{-6}	6.8×10^{-7}	NC	NC
CXCL1 [§]	0.01	0.001	7.2×10^{-6}	NC	NC
CXCL2 [†]	0.01	0.0016	5.8×10^{-4}	NC	NC
CXCL6 [†]	0.07	0.005	BDL	NC	NC

BDL, below detectable levels; NC, no significant change.

*Nanograms secreted per cell per 48 h.

[†]ELISA intra-assay variation <7.5%.

[‡]ELISA intra-assay variation <5%.

[§]ELISA intra-assay variation <10%.

Table S8. Cell counts from lesioned calvaria after 50 days of treatment

Treatment	Animal number			Mean	SD	<i>P</i> (Student's <i>t</i> test)
	1	2	3			
DMSO	235	141	206	194	48.13	Versus DMSO
BIO200	12	52	0	21.33	27.23	0.0057
BIO800	11	0	31	14	15.72	0.003
GW1.0	362	188	247	260.67	90.47	ns
GW10.0	341	215	232	262.67	68.36	ns

ns, not significant.